17. C. Salomon, talk presented at the Quantum Electronics and Laser Science Conference, Baltimore, MD, 5 June 2003.
18. T. Weber, J. Herbig, M. Mark, H.-C. Nägerl, R. Grimm, *Science* **299**, 232 (2003); published online 5 Dec 2002 (10.1126/science.1079699).
19. The optical trap has a depth of $k_B \times 45$ nK with a radial trap frequency of 18 Hz and an axial trap frequency of 6 Hz. The axial direction of the BEC is oriented in the horizontal plane. At 20 G, the Cs scattering length is $a = 163\ a_0$, with a_0 denoting Bohr's radius. The resulting chemical potential for the BEC is $k_B \times 7$ nK.
20. Materials and methods are available as supporting material on *Science* Online.
21. V. Vuletić, C. Chin, A. J. Kerman, S. Chu, *Phys. Rev. Lett.* **83**, 943 (1999).
22. P. S. Julienne, E. Tiesinga, private communication (2003).
23. C. Chin, V. Vuletić, A. J. Kerman, S. Chu, *Phys. Rev. Lett.* **85**, 2717 (2000).
24. P. J. Leo, C. J. Williams, P. S. Julienne, *Phys. Rev. Lett.* **85**, 2721 (2000).
25. The molecular state was identified as a high-lying rovibrational state with internal angular momentum $f = 4$, magnetic quantum number $m_f = 4$, molecular orbital angular momentum $L = 4$, and angular momentum projection $m_L = 2$.
26. T. Weber, J. Herbig, M. Mark, H.-C. Nägerl, R. Grimm, *Phys. Rev. Lett.*, in press (available at http://arXiv.org/abs/physics/0304052).
27. V. A. Yurovsky, A. Ben-Reuven, P. S. Julienne, C. J. Williams, *Phys. Rev. A* **62**, 043605 (2000).
28. This is a reasonable assumption, because no molecules can be created in the absence of atoms.
29. M. R. Andrews *et al.*, *Science* **275**, 637 (1997).
30. D. Jaksch, V. Venturi, J. I. Cirac, C. J. Williams, P. Zoller, *Phys. Rev. Lett.* **89**, 040402 (2002).
31. M. Greiner, O. Mandel, T. Esslinger, T. W. Hänsch, I. Bloch, *Nature* **415**, 39 (2002).

Cooling Bose-Einstein Condensates Below 500 Picokelvin

A. E. Leanhardt,* T. A. Pasquini, M. Saba, A. Schirotzek, Y. Shin, D. Kielpinski, D. E. Pritchard, W. Ketterle

Spin-polarized gaseous Bose-Einstein condensates were confined by a combination of gravitational and magnetic forces. The partially condensed atomic vapors were adiabatically decompressed by weakening the gravito-magnetic trap to a mean frequency of 1 hertz, then evaporatively reduced in size to 2500 atoms. This lowered the peak condensate density to 5×10^{10} atoms per cubic centimeter and cooled the entire cloud in all three dimensions to a kinetic temperature of 450 ± 80 picokelvin. Such spin-polarized, dilute, and ultracold gases are important for spectroscopy, metrology, and atom optics.

The pursuit of lower temperatures is motivated by the quest to observe phenomena that occur on very low energy scales, in particular, phase transitions to new forms of matter. The achievement of temperatures near 1 K in solids and in liquids led to the discoveries of superconductivity (*1*) and superfluidity (*2*), respectively. The advent of laser cooling resulted in microkelvin temperature atomic vapors (*3–5*), subsequently cooled to nanokelvin temperatures by evaporative cooling to form dilute Bose-Einstein condensates (*6*, *7*) and quantum degenerate Fermi gases (*8*). Collectively, these low-temperature systems have a host of applications, including superconducting quantum interference devices (SQUIDs) (*9*), superfluid gyroscopes (*10*, *11*), and atomic clocks (*12*).

Temperature is a quantity that parameterizes how energy is distributed across the available states of a system, and effective temperatures can be defined for decoupled degrees of freedom or subsets of particles. For example, nuclear spins isolated from the kinetic motion of their respective atoms have been cooled by adiabatic demagnetization to an effective temperature of 280 pK (*13*). Spin ensembles have a finite number of available states, such that a spin-polarized sample, as in our work, would be characterized by zero effective temperature. In contrast, the motion of free particles is subject to a continuum of states, and the kinetic temperature of an ensemble can only asymptotically approach absolute zero.

Effective temperatures in atomic vapors are defined by the widths of velocity distributions, which can be much smaller than the mean velocity of the sample. Raman cooling (*14*, *15*) and velocity-selective coherent population trapping (VSCPT) (*16*) have generated velocity distributions with very narrow peaks, corresponding to nanokelvin and picokelvin effective temperatures. However, these temperatures were associated with the motion of only a subset of the atoms in the cloud and/or with atomic motion in only one dimension.

For trapped, partially condensed atomic vapors, the condensate fraction has zero entropy and the kinetic temperature of the sample is determined by the velocity distribution of the thermal (noncondensed) component. When released, the condensate fraction expands more slowly than the thermal component and has been characterized by picokelvin effective temperatures for anisotropic (*17*) and noninteracting (*18*) gases.

Cooling the atomic motion of entire ensembles in all three dimensions has proven difficult. To date, kinetic temperatures of a few hundred nanokelvin have been achieved with adiabatic and optical cooling (*19*, *20*), and evaporative cooling techniques have produced condensates with temperatures of 3 nK (*21*). By adiabatic expansion and subsequent evaporation, we have cooled partially condensed atomic vapors to picokelvin kinetic temperatures.

Our thermometry is calibrated by the Bose-Einstein condensation (BEC) phase transition temperature, T_c, which in the thermodynamic limit for a harmonically trapped ideal Bose gas is (*22*)

$$k_B T_e = \hbar \bar{\omega} \left(\frac{N}{\zeta(3)} \right)^{1/3} \approx 0.94 \hbar \bar{\omega} N^{1/3} \qquad (1)$$

where k_B is Boltzmann's constant, $\hbar$ is Planck's constant h divided by 2π, $\zeta(n)$ is the Riemann Zeta function, $\bar{\omega} = (\omega_x \omega_y \omega_z)^{1/3}$ is the geometric mean of the harmonic trap frequencies, and N is the total number of atoms, both condensed and noncondensed. Thus, the atom number and the trap frequencies set an upper limit for the temperature of a confined Bose-Einstein condensate. In our work, adiabatically weakening the trapping potential to a mean frequency of $\bar{\omega} = 2\pi \times (1.12 \pm 0.08)$ Hz guaranteed that partially condensed atomic vapors with $N \leq 8000$ atoms had picokelvin temperatures ($T_c \leq 1$ nK).

Bose-Einstein condensates containing more than 10^7 ^{23}Na atoms were created in the weak field seeking $|F = 1, m_F = -1\rangle$ state in a magnetic trap, captured in the focus of an optical tweezers laser beam, and transferred into an auxiliary "science" chamber as described in (*23*). In the science chamber, condensates containing 2×10^6 to 3×10^6 atoms were transferred from the optical tweezers into a gravito-magnetic trap (Fig. 1A). A small coil carrying current I_S generated a vertical bias field B_z and supported the condensates against gravity with a vertical magnetic field gradient, $B'_z = 2\ mg/$

Department of Physics, MIT-Harvard Center for Ultracold Atoms, and Research Laboratory of Electronics, Massachusetts Institute of Technology, Cambridge, MA 02139, USA.

*To whom correspondence should be addressed. E-mail: ael@mit.edu

$\mu_B \approx 8$ G/cm, where m is the atomic mass, g is the gravitational acceleration, and μ_B is the Bohr magneton. Additional control over B_z and B'_z was provided by two external coils carrying independent currents I_U and I_L. Weak curvature, B'_z, to the vertical bias field created stable vertical confinement such that a harmonic restoring force was provided magnetically (gravitationally) for downward (upward) vertical displacements (Fig. 1B). A radial field gradient, $B'_r = \partial B_r / \partial r = -B'_z/2$, was also present and added in quadrature with B_z to provide harmonic radial confinement with a restoring force proportional to $(B'_r)^2/B_z$ (Fig. 1C). The trapping potential does not have fundamental radial asymmetries as do previously demonstrated Ioffe-Pritchard magnetic traps (17, 24, 25). In principle, stable three-dimensional confinement is possible above a single coil in the presence of gravity without the aid of external bias fields or gradients.

For typical loading parameters—$I_S = 340$ mA, $I_U = 5.5$ A, and $I_L = 0$—the gravito-magnetic trap was spherically symmetric, with trap frequencies $\omega_x \approx \omega_y \approx \omega_z \approx 2\pi \times 8$ Hz. Condensates loaded into the gravito-magnetic trap from the optical tweezers were held for 5 s to allow for the damping of excitations. The resulting partially condensed clouds had $\sim 5 \times 10^5$ atoms and a BEC transition temperature $T_c = 30$ nK. Throughout our work, the atomic vapor maintained a temperature T such that $0.5 < T/T_c < 1$.

Further cooling was accomplished by adiabatically decompressing the trapping potential in two 5 s stages, with a 5 s delay in between to allow excitations to damp. In the first stage, the vertical frequency was reduced to $\omega_z = 2\pi \times (1.81 \pm 0.05)$ Hz by simultaneously raising currents I_L and I_U by identical amounts and lowering the current I_S by a factor of 10. This transferred the dominant source of magnetic field gradient from the small coil to the external coils, with the remaining vertical curvature still due to the reduced I_S. In the second stage, the radial frequencies were reduced to $\omega_x = 2\pi \times (0.65 \pm 0.05)$ Hz and $\omega_y = 2\pi \times (1.2 \pm 0.1)$ Hz by raising I_L and lowering I_U by identical amounts. The vertical magnetic field gradient and curvature remained constant, but the vertical bias field, B_z, increased. This reduced the radial confinement due to the scaling $\omega_r \propto B'_r / B_z^{1/2}$ (24, 25).

For currents $I_S = 34$ mA, $I_U = 14$ A, and $I_L = 44$ A, the final gravito-magnetic trap had a measured mean frequency $\bar{\omega} = 2\pi \times (1.12 \pm 0.08)$ Hz and axial bias field $B_z = 17$ G. The residual anharmonicities of the trapping potential were small, with $\Delta\omega/\omega = 0.1$ for 500 μm displacements from the trap center. Further radial decompression was not possible because of a finite trap depth (Fig. 1C) and sensitivity of trap stability to milligauss level radial bias fields.
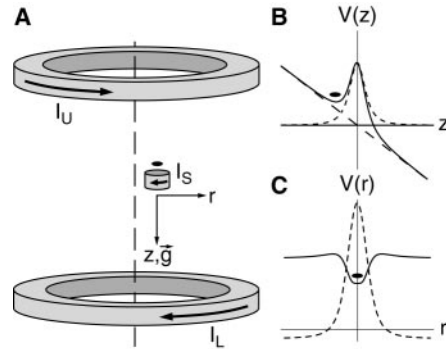
Fig. 1. Gravito-magnetic trap. (**A**) Bose-Einstein condensates were levitated against gravity $\sim$5 mm above a 1-cm diameter, 25-turn coil mounted inside the ultrahigh vacuum chamber running current I_S. Two 10-cm diameter, 20-turn coils were mounted outside the vacuum chamber and were supplied individually with currents I_U and I_L. The vertical separation between the large coils was 10 cm. The 1-cm diameter coil was mounted radially off-axis with respect to the pair of 10-cm diameter coils by $\sim$1 cm. This broke the cylindrical symmetry of the trapping potential. Additional bias fields of $\sim$1 G were applied in the horizontal plane to cancel the radial magnetic fields generated by I_U and I_L on the axis of the small coil and to maintain a stable trapping potential. $\vec{g}$ denotes the direction of gravitational acceleration. (**B**) Magnetic potential due to I_S (short dashed line), gravitation potential (long dashed line), and joint vertical potential of the gravito-magnetic trap (solid line). (**C**) A radially repulsive potential magnetic potential was generated by running I_S alone (dashed line); however, applying a slight antibias field with I_U modified the radial energy profile and created a magnetic field minimum at $r = 0$ (solid line). In (A) to (C), the solid oval denotes the trapped condensate.

After decompression, the partially condensed atomic vapors had $\sim 2 \times 10^5$ atoms and a BEC transition temperature $T_c = 3$ nK. T_c was lowered further by reducing the number of atoms in the cloud (Eq. 1), while maintaining a substantial condensate fraction at all times ($0.5 < T/T_c < 1$). The atom number was reduced by holding the atoms in the gravito-magnetic trap for up to 200 s. Often, microwave radiation near the $|1, -1\rangle \rightarrow |2, 0\rangle$ transition was applied to shorten the hold time required to arrive at lower atom number to 10 s. The atom number reduction was accompanied by cooling, during which the elastic collision rate (between thermal atoms and the condensate) dropped from 0.25 Hz to 0.01 Hz. Therefore, a few collisions were sufficient to cause evaporation out of the finite depth trap. This cooling was not efficient in the sense of providing a gain in phase-space density but still was capable of maintaining thermal equilibrium and lowering the absolute temperature of the vapor.

Using this technique, we cooled partially condensed vapors containing up to 30,000 atoms to temperatures below 1 nK (Figs. 2 and 3). Our lowest measured three-
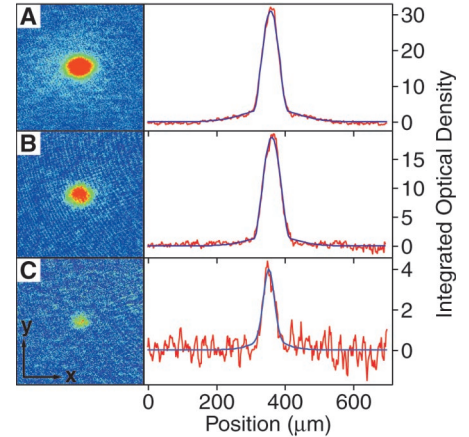
Fig. 2. Picokelvin temperature thermometry. Partially condensed atomic vapors confined in the gravito-magnetic trap with (**A**) 28,000, (**B**) 16,000, and (**C**) 2,500 atoms. The one-dimensional cross sections (red) were obtained by integrating the two-dimensional absorption images of the trapped clouds along the y axis. Bimodal fits to Eq. 2 (blue) yielded temperatures of (A) 1.05 ± 0.08 nK, (B) 780 ± 50 pK, and (C) 450 ± 80 pK, where the uncertainty is due to the fit of an individual image. The absorption imaging light was resonant with the $F = 2 \rightarrow F' = 3$ cycling transition for the trapped atoms and was aligned with the vertical (z) axis. The atoms were optically pumped into the $F = 2$ hyperfine level with a pulse resonant with the $F = 1 \rightarrow F' = 2$ transition. The field of view for the absorption images in (A) to (C) is 460 μm $\times$ 460 μm.

dimensional kinetic temperature was 450 ± 80 pK for 2500 atoms at a peak condensate density of 5×10^{10} atoms/cm^3. Under these conditions, the peak atom-atom interaction energy was $\mu = k_B \times 33$ pK, while the zero point energy of the harmonic trapping potential was $(1/2)\hbar\bar{\omega} k_B \times 24$ pK. Condensates released from the gravito-magnetic trap would expand with energies of this order and therefore could be characterized by effective temperatures $\sim$30 pK.

Additional cooling would require lowering the trap frequencies further or reducing the atom number more. However, weakly confining traps have proven technically difficult to control such that lowering $\bar{\omega}/2\pi$ substantially below 1 Hz is challenging. Likewise, because $T_c \propto N^{1/3}$, atom number reduction by an order of magnitude only results in temperature reduction by a factor of two. Furthermore, lower temperatures and lower densities are accompanied by collisional equilibrium times approaching 100 s.

Because $\mu \approx \hbar\bar{\omega}$, the condensates in the gravito-magnetic trap were in a density regime intermediate between the Thomas-Fermi ($\mu >> \hbar\bar{\omega}$) and ideal ($\mu << \hbar\bar{\omega}$) gas limits. No simple approximation describes the condensate wave function, but the number of thermal atoms, $N_{th} = \zeta(3) \times (k_B T \hbar\bar{\omega})^3$, and the width of their distribution,
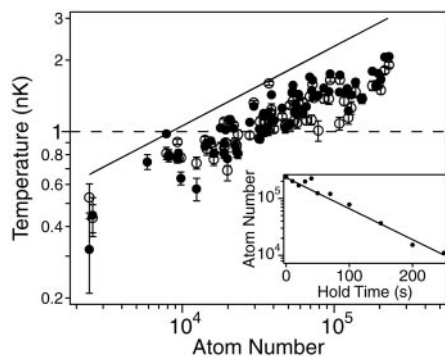
Fig. 3. Bose-Einstein condensates at picokelvin temperatures. The temperature of more than 60 partially condensed atomic vapors is plotted versus total number of condensed and noncondensed atoms. A solid line at the Bose-Einstein condensation phase transition temperature (Eq. 1) and a dashed line at 1 nK are provided as guides. Condensate temperatures were determined from one-dimensional fits to atomic density cross sections integrated along either the x (closed circles) or y (open circles) axis (Fig. 2). Differences in the two measured temperatures for a single condensate reflect the true uncertainty of the measurement. Plotted error bars represent the statistical uncertainty of the fit. The inset shows that the $1/e$ condensate lifetime in the gravito-magnetic trap was limited by one-body processes to 80 ± 5 s.

$w_{th} = (2k_B T / m\omega^2)^{1/2}$, in any spatial direction can be related to the temperature, provided that the thermal energy is much larger than the trap level spacing, $k_B T \gg \hbar \bar{\omega}$, where ω is the trap frequency for the axis along which w_{th} is measured (*22*). The ratio of atoms in the condensate, N_0, to the total number of atoms, $N = N_0 + N_{th}$, is also related to the temperature through $N_0/N = 1 - (T/T_c)^3$. N_0, N_{th}, and w_{th} are therefore completely determined by T and N.

The temperature of the atomic vapors was extracted by fitting integrated, one-dimensional atomic density cross sections to a bimodal distribution (Fig. 2)

$$n(x) = N_0\Psi_0^2 + \frac{N_{th}}{\sqrt{\pi} w_{th}} e^{-x^2/w_{th}^2} \quad (2)$$

where Ψ_0^2 is a bell-shaped function with width w_0 that describes the condensate peak $[\Psi_0^2 = (15/16) w_0^{-1} \max(1 - x^2/w_0^2, 0)^2$ for a Thomas-Fermi gas and $\Psi_0^2 = w_0^{-1}\pi^{-1/2} \exp(-x^2/w_0^2)$ for an ideal gas]. The fitted parameters were T, N, and w_0. We checked that the fitted temperature did not depend on the exact choice of the condensate wave function (inverted parabola or gaussian) or the application of microwave radiation to reduce atom number.

All atomic vapors represented in Fig. 3 had a clear bimodal density distribution from which a temperature was reproducibly extracted. The temperatures extracted from one-dimensional fits along both radial axes were nominally the same, empirically indicating that the atomic vapors remained close to thermal equilibrium at all times.

In conclusion, we have created long-lived (80 ± 5 s), low-temperature (450 ± 80 pK), and low-density (5×10^{10} atoms/cm³) partially condensed atomic vapors using a weakly confining [$\varpi = 2\pi \times (1.12 \pm 0.08)$ Hz] gravito-magnetic trap. These samples are characterized by a thermal velocity ~1 mm/s, a speed of sound ~100 μm/s, and a healing length limited by the ~20-μm harmonic oscillator length of the trapping potential. Low-temperature and low-density ensembles are important for spectroscopy, metrology, and atom optics. In addition, they are predicted to experience quantum reflection from material surfaces (*26–28*).

References and Notes
1. H. G. Smith, J. O. Wilhelm, *Rev. Mod. Phys.* **7**, 237 (1935).
2. K. Darrow, *Rev. Mod. Phys.* **12**, 257 (1940).
3. S. Chu, *Rev. Mod. Phys.* **70**, 685 (1998).
4. C. N. Cohen-Tannoudji, *Rev. Mod. Phys.* **70**, 707 (1998).
5. W. D. Phillips, *Rev. Mod. Phys.* **70**, 721 (1998).
6. E. A. Cornell, C. E. Wieman, *Rev. Mod. Phys.* **74**, 875 (2002).
7. W. Ketterle, *Rev. Mod. Phys.* **74**, 1131 (2002).
8. B. DeMarco, D. S. Jin, *Science* **285**, 1703 (1999).
9. A. H. Silver, J. E. Zimmerman, *Phys. Rev. Lett.* **15**, 888 (1965).
10. K. Schwab, N. Bruckner, R. E. Packard, *Nature* **386**, 585 (1997).
11. O. Avenel, P. Hakonen, E. Varoquaux, *Phys. Rev. Lett.* **78**, 3602 (1997).
12. T. Udem, R. Holzwarth, T. W. Hänsch, *Nature* **416**, 233 (2002).
13. A. S. Oja, O. V. Lounasmaa, *Rev. Mod. Phys.* **69**, 1 (1997).
14. M. Kasevich, S. Chu, *Phys. Rev. Lett.* **69**, 1741 (1992).
15. J. Reichel *et al.*, *Phys. Rev. Lett.* **75**, 4575 (1995).
16. B. Saubaméa *et al.*, *Phys. Rev. Lett.* **79**, 3146 (1997).
17. M.-O. Mewes *et al.*, *Phys. Rev. Lett.* **77**, 416 (1996).
18. T. Weber, J. Herbig, M. Mark, H.-C. Nägerl, R. Grimm, *Science* **299**, 232 (2003).
19. A. Kastberg, W. D. Phillips, S. L. Rolston, R. J. C. Spreeuw, *Phys. Rev. Lett.* **74**, 1542 (1995).
20. P. Treutlein, K. Y. Chung, S. Chu, *Phys. Rev. A* **63**, 051401(R) (2001).
21. E. A. Donley, N. R. Claussen, S. T. Thompson, C. E. Wieman, *Nature* **417**, 529 (2002).
22. F. Dalfovo, S. Giorgini, L. P. Pitaeskii, S. Stringari, *Rev. Mod. Phys.* **71**, 463 (1999).
23. T. L. Gustavson *et al.*, *Phys. Rev. Lett.* **88**, 020401 (2002).
24. Y. V. Gott, M. S. Ioffe, V. G. Tel'kovskii, *Nuc. Fus. Suppl.* **3**, 1045 (1962).
25. D. E. Pritchard, *Phys. Rev. Lett.* **51**, 1336 (1983).
26. A. Anderson *et al.*, *Phys. Rev. A* **34**, 3513 (1986).
27. J. J. Berkhout *et al.*, *Phys. Rev. Lett.* **63**, 1689 (1989).
28. F. Shimizu, *Phys. Rev. Lett.* **86**, 987 (2001).
29. This work was funded by the Army Research Office, NSF, Office of Naval Research, and NASA. We thank C. V. Nielsen for experimental assistance and J. K. Thompson for critical comments on the manuscript. M.S. acknowledges additional support from the Swiss National Science Foundation.

Observation of Polymer Conformation Hysteresis in Extensional Flow

Charles M. Schroeder,[1] Hazen P. Babcock,[2]* Eric S. G. Shaqfeh,[1,3] Steven Chu[2]†

Highly extensible *Escherichia coli* DNA molecules in planar extensional flow were visualized in dilute solution by fluorescence microscopy. For a narrow range of flow strengths, the molecules were found in either a coiled or highly extended conformation, depending on the deformation history of the polymer. This conformation hysteresis persists for many polymer relaxation times and is due to conformation-dependent hydrodynamic forces. Polymer conformational free-energy landscapes were calculated from computer simulations and show two free-energy minima for flow strengths near the coil-stretch transition. Hysteresis cycles may directly influence bulk-solution stresses and the development of stress-strain relations for dilute polymer flows.

The behavior of long-chain, flexible polymer molecules in extension-dominated flows has been the subject of research discussion for more than 30 years (*1*). Flows of dilute polymer solutions exhibit several interesting macroscopic effects including flow-dependent viscosity, enhanced normal stresses, and turbulent-drag reduction. Such non-Newtonian fluid properties result from flow-induced changes in the polymer conformations in solution. In short, a flowing fluid will influence polymer configurations in solution, and the forces exerted back on the fluid are directly related to the molecular conformations.

Polymer conformations and the resultant bulk-solution stresses are affected by flow type. In general, flows with a large rotational

[1]Department of Chemical Engineering, [2]Departments of Physics and Applied Physics, [3]Department of Mechanical Engineering, Stanford University, Stanford, CA 94305, USA.

*Present address: Department of Chemistry and Chemical Biology, Harvard University, Cambridge, MA 02138, USA.
†To whom correspondence should be addressed. E-mail: schu@stanford.edu